Molecular Catalysis xxx (xxxx) xxx–xxx

Contents lists available at ScienceDirect

Molecular Catalysis

journal homepage: www.elsevier.com/locate/mcat

Solvent effects in solid acid-catalyzed reactions: The case of the liquid-phase isomerization/cyclization of citronellal over SiO_2-Al_2O_3

Nicolás M. Bertero*,[1], Andrés F. Trasarti, María C. Acevedo, Alberto J. Marchi, Carlos R. Apesteguía*,[1]

Catalysis Science and Engineering Research Group (GICIC), INCAPE, UNL-CONICET, CCT Conicet- Paraje El Pozo, 3000, Santa Fe, Argentina

ARTICLE INFO

Keywords:
Solvent effect
Citronellal isomerization/cyclization
Isopulegol
Fine chemistry
SiO_2-Al_2O_3

ABSTRACT

The effect of solvent on the activity and selectivity of SiO_2-Al_2O_3 in the liquid-phase acid-catalyzed isomerization/cyclization of citronellal (CNAL) to isopulegol was investigated using non-polar (cyclohexane, toluene), weakly polar (chloroform), polar protic (ethanol, 2-propanol) and polar aprotic (acetonitrile) solvents. The catalyst activity and selectivity greatly depended on the solvent nature. The CNAL conversion rate was higher in weakly and non-polar (chloroform > toluene > cyclohexane) than in polar solvents (ethanol > acetonitrile > 2-propanol). To interpret this activity pattern, the solvent-CNAL interactions were analyzed by measuring the shift of the infrared C=O absorption band of CNAL in CNAL/solvent mixtures, while the solvent-catalyst interactions were characterized by both determining the solvent adsorption enthalpies by calorimetry and following the product evolution from temperature-programmed desorption of solvents. In the case of polar solvents, both the strong solvation effect in the liquid phase and the adsorption strength of solvents on SiO_2-Al_2O_3 contributed to decrease the catalyst isomerization activity. In particular, the selectivity to isopulegol was clearly lower in polar protic solvents (ethanol and 2-propanol) because secondary reactions producing carbon deposits took place. In contrast, in non-polar solvents the selectivity to isopulegol was higher than 97% in all the cases. The highest isomerization rate was obtained in chloroform that partially adsorbs dissociatively on SiO_2-Al_2O_3, leading to a higher density of acid sites available for the isomerization reaction.

1. Introduction

In fine chemistry, the technological optimization of liquid-phase catalytic processes promoted by solid catalysts requires the development of active and selective catalysts, the use of proper reactor operating conditions and the correct choice of the solvent. Nevertheless, the impact of solvent on catalyst activity and selectivity has been little investigated in heterogeneous catalysis in spite that the solvent nature may greatly influence the catalyst performance [1–3]. Optimal solvent selection is not straightforward because a detailed knowledge on the relationship between the solvent nature and the gas-liquid-solid interactions taking place in slurry reactors is required to take a proper decision. An exhaustive analysis of reactor data based on scientific principles is therefore needed to better predict the solvent effect on catalyst performance. Furthermore, experimental runs should be performed in a significant number of different solvents in order to reach valid conclusions for a wide range of solvent properties.

In previous works, the effect of solvent on the activity and selectivity of metal-supported catalysts for the liquid-phase hydrogenation of aromatic ketones [4,5] and nitriles [6–8] was studied on several metal-based catalysts (Ni, Co, Cu, Pt, Pd, Ru) using different solvent groups (polar, non-polar, protic and aprotic solvents). These studies showed that the solvent chemical nature may dramatically affect the catalyst activity and selectivity for liquid-phase hydrogenation reactions. For example, strong solvent adsorption on the catalyst surface may partially (or totally) block the metal active sites for reactant adsorption and thereby decreasing the catalyst activity. In the liquid phase, the reactant solvation increases with the strength of reactant-solvent interaction and may impact on the catalytic activity by hampering the reactant adsorption on the catalyst surface.

In the present work, we study the effect of solvent in solid acid-catalyzed reactions by using the citronellal (CNAL) isomerization/cyclization to isopulegol (IP) as a model reaction (Scheme 1). Conversion of CNAL to IP is an isomerization reaction since both compounds have the same molecular formula ($C_{10}H_{18}O$) and, at the same time, is a cyclization reaction because IP is a cyclic product. For simplicity, from

* Corresponding authors at: INCAPE, Predio CCT Conicet, Paraje El Pozo, 3000 Santa Fe, Argentina.
E-mail addresses: nbertero@fiq.unl.edu.ar (N.M. Bertero), capesteg@fiq.unl.edu.ar (C.R. Apesteguía).
[1] Website: http://www.fiq.unl.edu.ar/gicic.

https://doi.org/10.1016/j.mcat.2018.09.009
Received 29 June 2018; Received in revised form 31 August 2018; Accepted 6 September 2018

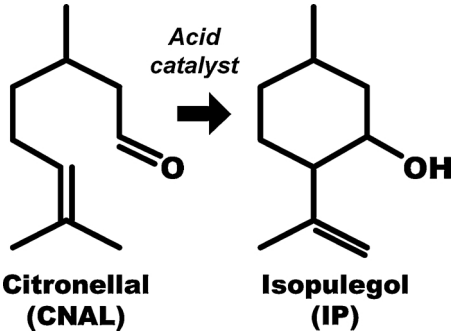

Scheme 1. Isomerization/cyclization of citronellal to isopulegol.

now on, it will be identified as an *isomerization* reaction. This reaction has been widely studied using liquid and solid acid catalysts because it is involved in the reaction network for the synthesis of menthols [9,10]. In heterogeneous catalysis, the liquid-phase citronellal isomerization to isopulegol was extensively investigated on acid zeolites, such as zeolites HY, MCM-22, ZSM5 and HBEA, as well as on supported heteropolyacids, sulfated zirconia and titania, SiO_2-Al_2O_3, Al-MCM-41 and other solid acids [11–17]. However, few papers have been published on the effect of solvent on the catalyst performance for this reaction. Coman et al. [18] studied the citronellal isomerization on metal fluorides in non-polar (toluene, cyclohexane and n-heptane) and polar (2-propanol) solvents and found that the catalyst activity was higher in non-polar solvents than in 2-propanol. They attributed the lower reaction rates obtained in 2-propanol to a strong adsorption of the solvent on the catalyst Lewis acid sites that renders the active sites inaccessible to substrates. Consistently, Müller et al. [19] observed that citronellal isomerization was faster in non-polar toluene than in polar acetonitrile over SBA-15, Sn-SBA-15 and Sn-SiO_2. In contrast, Yongzhong et al. [20] reported that the citronellal conversion rate was faster in polar solvents 2-propanol, acetonitrile and 2-butanol than in non-polar solvents toluene and cyclohexane over Zr-zeolite beta.

Analysis of publications on the solvent effect for citronellal isomerization shows that the studies were carried out using a small number of solvents and, as a consequence, a general understanding of the relationship between the solvent characteristic and the catalyst performance is lacking. Here, we investigated the solvent effect on catalyst activity and selectivity for the liquid-phase isomerization of citronellal to isopulegol over SiO_2-Al_2O_3 using six solvents of different properties and polarities: 1) cyclohexane (CHX) and toluene (TOL) are non-polar solvents; 2) chloroform (CLF) is a weakly polar solvent; 3) ethanol (EtOH) and 2-propanol (2-PrOH) are polar protic solvents; 4) acetonitrile (ACN) is a polar aprotic solvent. The selection of the catalyst for this study was based on the following requirements: a) high density of Lewis and Brønsted acid sites; b) high stability during the liquid phase reaction, without leaching; c) high specific surface area in order to promote solvent-catalyst and reactant-catalyst interactions; d) porous structure based on macro or mesopores in order to avoid intraparticle mass transfer limitations. In this study SiO_2-Al_2O_3 was selected to carrying out the reaction because is an efficient catalyst for CNAL isomerization [12,16] and fulfills the previous requirements. Data analysis by considering the solvent-reactant, solvent-catalyst, and solvent-reactant-catalyst interactions allowed us to interpret and explain the solvent influence on catalyst performance on the basis of the solvent properties.

2. Experimental

2.1. Materials

SiO_2-Al_2O_3 Grade 135 (99% Aldrich), citronellal (≥95.0% Aldrich), 2-propanol (anhydrous 99.5% Sigma-Aldrich), cyclohexane (anhydrous 99.5% Sigma-Aldrich), toluene (anhydrous, 99.8% Sigma-Aldrich), ethanol (anhydrous ≥99.8% Sigma-Aldrich), acetonitrile (anhydrous 99.8% Sigma-Aldrich), and chloroform (≥99% Sigma-Aldrich), n-dodecane (99% Sigma).

2.2. Catalyst characterization

Elemental compositions were determined by atomic absorption spectroscopy using a Perkin-Elmer 3110 spectrophotometer. Surface areas and pore volumes were measured by N_2 physisorption at −196 °C in a Quantachrome Nova-1000 sorptometer using the BET method and Barret-Joyner–Halender (BJH) calculations, respectively. The particle size distribution was determined with a Camsizer XT particle analyzer (Retsch Technology). In all the cases, the X-Jet dipersion module was employed at 10 kPa air dispersion pressure.

Sample acid properties were probed by temperature-programmed desorption (TPD) of NH_3 preadsorbed at 100 °C. Calcined samples (150 mg) were treated in Ar (60 mL min^{-1}) at 200 °C for 1 h and then exposed to a 1% NH_3/He stream for 45 min at 100 °C. Weakly adsorbed NH_3 was removed by flowing Ar at 100 °C for 2 h. The temperature was then increased at 10 °C min^{-1} and the NH_3 concentration in the effluent was measured by mass spectrometry in a Baltzers Omnistar unit.

Coke formed on the catalysts during reaction was measured by temperature-programmed oxidation (TPO). Samples (20 mg) were initially treated in N_2 flow for 1 h at 100 °C to eliminate weakly adsorbed molecules of reactants or products. Then, samples were heated in a 2% O_2/N_2 molar stream at 10 °C min^{-1} from 25 °C to 800 °C. The evolved CO_2 was converted into methane in a fixed bed reactor containing a methanation catalyst (Ni/kieselguhr) at 400 °C. Then, methane was analyzed in a SRI 8610C gas chromatograph equipped with a flame ionization detector.

The nature and density of surface acid sites were determined by Fourier-transform infrared spectroscopy (FTIR) in a Shimadzu FTIR-8101 M spectrophotometer using pyridine as a probe molecule. Samples were ground to a fine powder and pressed into wafers (20–40 mg) at 5 ton cm^{-2}. The discs were mounted in a quartz sample holder and transferred to an inverted T-shaped Pyrex cell equipped with CaF_2 windows. Samples were outgassed in vacuum at 450 °C K during 4 h and then a background spectrum was recorded after being cooled down to room temperature (RT). Data were obtained at RT, after admission of pyridine and degassing at 150 °C, 300 °C, and 450 °C for 30 min. Spectra were recorded by subtracting the background spectrum. The spectral resolution was 2 cm^{-1} and the spectra are the average of 50 scans.

2.3. Solvent-citronellal interactions

Solvent-CNAL interactions were investigated by FTIR. Solvent/CNAL mixtures of C_{CNAL} = 0.143 M were analyzed in the 7500-370 cm^{-1} region with spectral resolution of 0.1 cm^{-1}. A Bruker Equinox 55 FT-IR spectrophotometer equipped with a DLATGS detector, KBr windows, and mechanical interferometer with ROCKSOLID^M alignment, was used.

2.4. Calorimetric determinations

Enthalpies of solvent adsorption on SiO_2-Al_2O_3 were determined by mixing 5 g of sample with 20 mL of solvent in a calorimeter equipped with mechanical stirrer and digital thermometer ERTCO-EUTECHNICS 4400 (0.01 °C resolution). *n*-dodecane (Sigma 99%, 40 mL) was used as calorimetric fluid. The calorimeter constant was determined by mixing bidistilled water and absolute ethanol; the ethanol molar fraction in the final mixture was 0.05. The corrected temperature rise, due to lack of adiabatic conditions and frictional dissipation of the stirring, was determined from the obtained thermograms by the Dickinson method [21].

2.5. Temperature-programmed desorption experiments

Solvent-catalyst interactions were investigated by TPD of solvents preadsorbed at RT. SiO_2-Al_2O_3 samples (150 mg) were heated in Ar at 200 °C for 1 h and then cooled down to RT. Afterwards, the sample was exposed to a solvent-saturated Ar stream for 15 min following the effluent composition by mass spectrometry in a Baltzers Omnistar unit. The weakly adsorbed solvent was removed by flushing with Ar (60 mL min^{-1}) at RT for 1 h. Temperature was then increased at a rate of 10 °C min^{-1} up to 600 °C and the composition of the reactor effluent was measured by mass spectrometry.

2.6. Catalytic tests

The liquid-phase isomerization of citronellal was carried out in a batch reactor (Parr 4843) at 70 °C and 5 bar (N_2). The reactor was loaded under N_2 atmosphere with 150 mL of solvent, 0.2 g of catalyst (previously calcined in air at 500 °C for 2 h) and 1 mL of n-dodecane as internal standard. The reaction system was stirred at 700 rpm and heated slowly up to 70 °C; then, 4 mL of citronellal were added to the autoclave and the N_2 pressure was rapidly increased to 5 bar to start the reaction. In all the cases, the initial citronellal concentration was 0.143 M. Product concentrations were analyzed by ex-situ gas chromatography using an Agilent 6850 GC chromatograph equipped with flame ionization detector, temperature programmer and a HP-1 capillary column (50 m × 0.32 mm ID, 1.05 µm film). Samples from the reaction system were taken by using a loop under pressure to avoid flashing. Data were collected every 15–60 min for 300 min. In all the catalytic experiments, the only products detected in liquid phase were the isopulegol isomers, i.e. isopulegol, neo-isopulegol, iso-isopulegol, neoiso-isopulegol. In all the cases, the isomer ratios were close to those predicted by thermodynamic equilibrium, i.e. isopulegol:neo-isopulegol:iso-isopulegol:neoiso-isopulegol = 63:26:8:3. Here, we note as *isopulegol* (IP) the sum of isopulegol isomers.

The significance of gas-liquid, liquid-solid and intraparticle mass transfer on the kinetic regime for the reaction operating conditions used in this work (stirring speeds of 700 rpm and particle diameters lower than 150 µm) was investigated by applying the quantitative criterion described by Ramachandran and Chaudhari [22]. The absence of intraparticle diffusion limitations was also checked by using the Weisz-Prater criterion [23]. Details of these calculations are presented in the Supplementary Information (Section SI.1). Based on the above analysis, it was verified that the kinetic data presented here were obtained under chemical regime.

The conversion of citronellal was calculated as $X_{CNAL} = \frac{(C^0_{CNAL} - C_{CNAL})}{C^0_{CNAL}}$, where C^0_{CNAL} is the initial concentration of citronellal and C_{CNAL} is the concentration of citronellal at time *t*. The yield to isopulegol (η_{IP}, mol of isopulegol/mol of citronellal fed) was determined as $\eta_{IP} = C_{IP}/C^0_{CNAL}$ where C_{IP} is the isopulegol concentration at time t. The selectivity to isopulegol (S_{IP}, mol of isopulegol/mol of citronellal reacted) was calculated as $S_{IP} = \eta_{IP}/X_{CNAL}$. The carbon balance at time *t* (%*C*) was determined as $\%C = \frac{(C_{IP} + C_{CNAL})}{C^0_{CNAL}}$. 100.

3. Results

3.1. Characterization of SiO_2-Al_2O_3

The Si/Al ratio of the SiO_2-Al_2O_3 sample used in this work was 7. The SiO_2-Al_2O_3 textural properties (surface area and pore size distribution) were obtained from the adsorption/desorption isotherms of N_2 obtained at −196 °C and are shown in the Supplementary Information (Fig. SI.1a). The surface area determined from the N_2 adsorption isotherm by applying the BET method was 462 m^2 g^{-1}. The pore size showed a bimodal distribution (Fig. SI.1b) with the maximum at 50 Å and a shoulder at 100 Å. The sample pore volume obtained by using BJH calculations was 0.74 cm^3 g^{-1}.

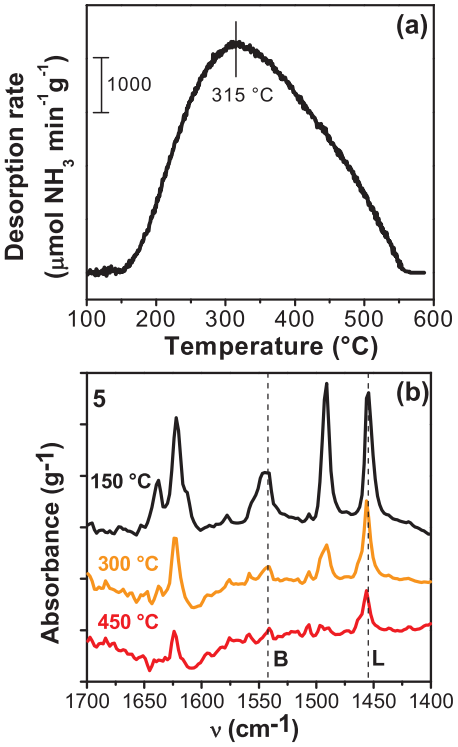

Fig. 1. Characterization of SiO_2-Al_2O_3 acidity: (a) TPD of NH_3 (preadsorbed at 100 °C); (b) FTIR spectrum of pyridine (preadsorbed at RT and degassing at 150 °C, 300 °C, and 450 °C; B: Brønsted, L: Lewis).

The particle size distribution of SiO_2-Al_2O_3 determined by dynamic image analysis is presented in Fig. SI.2. Particle sizes were lower than 150 µm (Fig. SI.2a) while the average particle size was 62 µm (Fig. SI.2b). The obtained D-values were D10 = 38.4 µm, D50 = 63.8 µm and D90 = 97.9 µm.

The density and strength of surface acid sites were probed by TPD of NH_3 preadsorbed at 100 °C; the obtained TPD curve is shown in Fig. 1a. The evolved NH_3 from SiO_2-Al_2O_3 sample gave rise to a broad band between 150 °C and 600 °C with a maximum around 240 °C. The acid site density obtained by deconvolution and integration of the NH_3 TPD trace in Fig. 1a was 380 µmol g^{-1}. The nature and strength of acid sites on SiO_2-Al_2O_3 was determined by FTIR of adsorbed pyridine after admission at RT and degassing at 150 °C, 300 °C and 450 °C. Fig. 1b shows the IR spectra obtained in the 1400-1700 cm^{-1} region for pyridine adsorbed on SiO_2-Al_2O_3. The pyridine absorption band at around 1545 cm^{-1} is characteristic for pyridinium ions adsorbed on Brønsted acid sites (B), while the band at 1455 cm^{-1} accounts for coordinately bound pyridine on Lewis acid sites (L) associated with tricoordinate Al atoms [24,25]. The relative contribution of Lewis and Brønsted acid sites was obtained then by deconvolution and integration of pyridine absorption bands at 1455 cm^{-1} and 1545 cm^{-1}, respectively. A value of L/(L + B) = 0.79 was obtained from the spectrum obtained after degassing at 150 °C. After degassing at 450 °C, the band at 1455 cm^{-1} was still present while that at 1545 cm^{-1} was negligible, thereby indicating that SiO_2-Al_2O_3 contains strong Lewis and weak Brønsted acid sites.

3.2. Catalytic tests

Fig. 2 shows the X_{CNAL} evolution as a function of time for all the solvents used in this work. From the results in Fig. 2, it is clear that the SiO_2-Al_2O_3 activity for CNAL isomerization was strongly influenced by the solvent employed to carry out the reaction. Quantitative data obtained from catalytic tests are given in Table 1. Specifically, Table 1

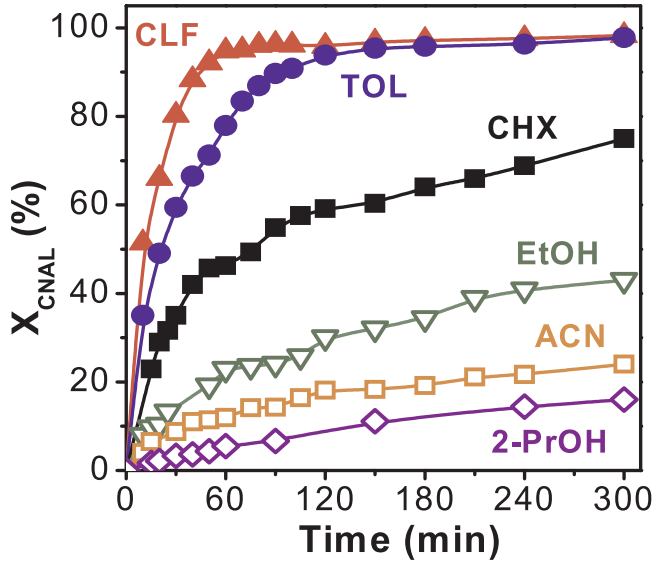

Fig. 2. Solvent effect on citronellal conversion over SiO_2-Al_2O_3 [T = 70 °C, P_{N_2} = 5 bar, W_{Cat} = 0.2 g, C^0_{CNAL} = 0.143 M, V_{CNAL}:V_{Solv} = 4:150 (mL)].

presents the initial CNAL conversion rates (r^0_{CNAL}, mmol min^{-1} g^{-1}), and the values of X_{CNAL}, η_{IP}, S_{IP} and %C obtained at the end of the runs. The r^0_{CNAL} values were determined from the experimental curves of Fig. 2 by polynomial regression and numerical differentiation at $t = 0$. Inspection of the results in Fig. 2 and Table 1 allow us to distinguish between two groups of solvents: i) X_{CNAL} was higher than 70% at the end of the runs when the reaction was performed in CLF, TOL and CHX (Table 1, entries 1–3); ii) X_{CNAL} was lower than 50% in EtOH, ACN and 2-PrOH (Table 1, entries 4–6). The solvents used in this work may be classified, according to their values of dielectric constant (ε) and dipole moment (μ) [26], in two categories: i) non-polar and weakly polar solvents (CHX, TOL and CLF), and ii) strongly polar solvents (EtOH, 2-PrOH and ACN). Regarding the effect of solvent on CNAL conversion rates, data in Table 1 show that r^0_{CNAL} follows the order CLF > TOL > CHX for weakly and non-polar solvents and EtOH > ACN > 2-PrOH for polar solvents.

Data in Table 1 also show that the selectivity to isopulegol depended on the solvent used. In fact, S_{IP} was close to 100% in weakly and non-polar solvents and in ACN, while in polar protic solvents 2-PrOH and EtOH it reached only 58.7% and 11.8%, respectively. On the other hand, the carbon balance at the end of reaction was higher than 97% in all the solvents excepting 2-PrOH (%C = 93%) and EtOH (%C = 63%).

In summary, results presented in Fig. 2 and Table 1 clearly show that the solvent selection is crucial for obtaining high citronellal isomerization rates in liquid phase. For example, r^0_{CNAL} in CLF was more than 30 times higher than in 2-PrOH (Table 1). In an attempt of explaining the strong effect of solvent on catalyst activity, we investigated the different solvent interactions between CNAL and the catalyst in the reaction system, i.e. solvent-CNAL, solvent-catalyst, and solvent-CNAL-catalyst interactions.

3.3. Catalyst activity and solvent-CNAL interactions in the liquid phase

3.3.1. Analysis based on solvent polarity parameters

To interpret the effect of solvent on catalyst activity in liquid-phase reactions, many authors have tried to correlate the reaction rates values with classical solvent polarity parameters, i.e. dipolar moment (μ) and dielectric constant (ε_D). However, both parameters provide little information about the ability of the solvent molecule to interact with the reactant molecule at a close range [27]. Thus, other parameters, such as solvatochromic scales of polarity that reflect better the solvent-reactant interactions at molecular level have been employed to predict the solvation properties of a solvent and to elucidate the solvent effect on catalyst activity [28]. In this work, we have investigated the influence of solvent-reactant interactions by plotting the CNAL isomerization rate against classical polarity parameters (μ and ε_D) and several solvatochromic scales such as hydrogen-bond donor (α) and hydrogen-bond acceptor (β) parameters, π* polarity/polarizability index, Kosower's Z and E_T(30) scales. The definition and significance of these parameters as well as their values for the solvents used in this work are given in Supplementary Information (Table SI.3).

The plots of initial CNAL isomerization rates against the solvent polarity parameters are presented in Fig. 3. Results in Fig. 3 show that no linear or monotonic correlation exists between r^0_{CNAL} and the solvent polarity parameters. By analyzing separately in the graphical representations of Fig. 3 the experimental points according to the solvent type (polar and non-polar solvents), we observe that when the reaction was carried out in weakly and non-polar solvents CLF, TOL and CHX, r^0_{CNAL} increased by a factor of about three from CHX to CLF, even though there are no important differences among the polarity/polarizability parameters of the three solvents (Table SI.3). In contrast, the r^0_{CNAL} value was similar in polar solvents 2-PrOH, ACN and EtOH in spite that the solvent polarity changed significantly (see Fig. 3a–d).

In summary, no proper correlation between r^0_{CNAL} and solvent polarity parameters is observed in Fig. 3 for the whole series of polar and non-polar solvents used in this work. Solvatochromic scales of solvent polarity are based on shifts in the absorption spectrum of a reference dye. The shifts in the maxima of the charge-transfer bands reflect the solvent effect on the energy gap between the ground state and the excited state of the reference dye molecule. The Kosower's Z and the E_T(30) solvatochromic scales are based on the absorption spectra of 1-ethyl-4-carbomethoxypyridinium iodide and pyridinium N-phenol betaine dyes, respectively [28,29]. It is worth noting that the nature of the solvent-dye interaction is different from that of solvent-CNAL, and thus these solvatochromic scales may not necessarily predict the solvent nature effect on solvent-CNAL interactions. In order to gain a better understanding of the effect of solvent-reactant interactions on catalyst activity, we investigated the direct solvent-CNAL interaction by FTIR

Table 1
Citronellal isomerization over SiO_2-Al_2O_3: Catalytic results.

Entry	Solvent	Initial reaction rate r^0_{CNAL} (mmol min^{-1} g^{-1})	Conversion [a] X_{CNAL} (%)	Yield [a] η_{IP} (%)	Selectivity [a] S_{IP} (%)	C balance [a] %C (%)
1	CLF	6.2	98.6	96.3	97.7	97.7
2	TOL	5.1	98.4	97.2	98.8	98.8
3	CHX	2.3	74.2	72.5	97.7	98.3
4	EtOH	1.1	42.5	5.4	11.8	62.9
5	ACN	0.6	25.3	25.3	100.0	100.0
6	2-PrOH	0.2	17.2	10.1	58.7	92.9

T = 70 °C, P_{N_2} = 5 bar, C^0_{CNAL} = 0.143 M, W_{Cat} = 0.2 g, V_{Solv} = 150 ml.
[a] At the end of 5-h catalytic runs.

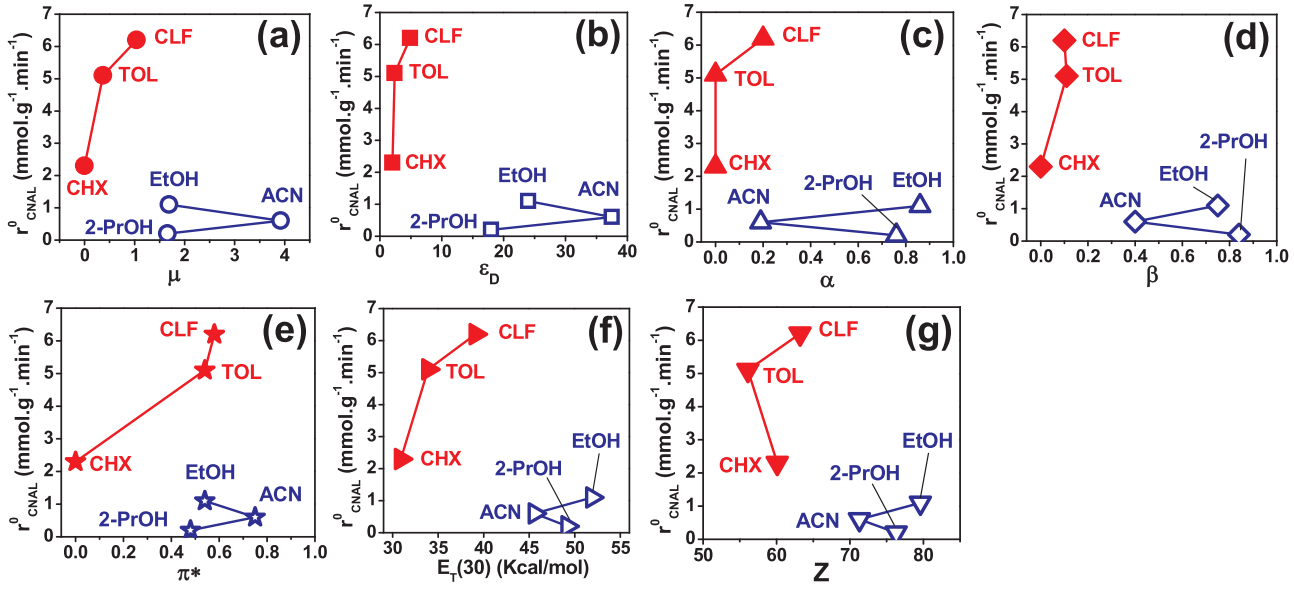

Fig. 3. Initial CNAL conversion rate as a function of dipole moment μ (a), dielectric constant ε_D (b), hydrogen-bond donor parameter α (c), hydrogen-bond acceptor parameter β (d), polarity/polarizability parameter π* (e), and solvatochromic parameters E_T(30) (f) and Z (g) [Catalyst: SiO_2-Al_2O_3, T = 70 °C, P_{N_2} = 5 bar, W_{Cat} = 0.2 g, C^0_{CNAL} = 0.143 M, V_{CNAL}:V_{Solv} = 4:150 (mL)].

technique.

3.3.2. Study of citronellal-solvent interactions by FTIR

Solvation involves the formation of a set of interactions between a solute and a solvent as well as a change in the interactions of the solvent molecules in the vicinity of the solute. The application of IR spectroscopy is a simple and convenient method for investigating solvent-solute interactions because the solvent polarity may induce significant shifts in the position of the IR absorption bands corresponding to solute functional groups. The carbonyl stretching vibrations, $\nu_{C=O}$, of a wide range of compounds in many solvents were determined in pioneer works and it was observed that the $\nu_{C=O}$ shifts seem to be produced mainly by local association effects with the solvent rather than by dielectric constant factors [30–32]. In particular, the IR spectra of aldehyde molecules such as citronellal exhibit the absorption band characteristics of the carbonyl stretching vibration in the 1740–1655 cm^{-1} region. Here, we obtained the IR spectra for pure citronellal and solvent-citronellal mixtures in the 1650-1800 cm^{-1} region and measured the $\nu_{C=O}$ peak position arising from citronellal. Results are given in Table 2. The peak maximum of $\nu_{C=O}$ band for pure CNAL appeared at 1725.3 cm^{-1}. The difference between the $\nu_{C=O}$ values determined for CNAL and a given CNAL-solvent mixture ($\Delta\nu_{C=O}$, cm^{-1}) provides information about the nature and strength of CNAL-solvent interaction. An upward or blue shift of $\nu_{C=O}$ was observed when CNAL was dissolved in non-polar solvents TOL ($\Delta\nu_{C=O}$ = 2.0 cm^{-1}) and CHX ($\Delta\nu_{C=O}$ = 6.5 cm^{-1}), thereby indicating a low CNAL-solvent interaction strength. These non-polar solvents have not capability to act as H-bond donors (α = 0 for TOL and CHX, Table SI.3) and they can interact with CNAL only via non-specific induction and dispersion forces. Thus, CNAL dilution by the addition of TOL or CHX would decrease the interaction between CNAL molecules and, as a consequence, the vibration frequency of the carbonyl group increases. In contrast, a downward shift of $\nu_{C=O}$ was verified for the CNAL-CLF mixture ($\Delta\nu_{C=O}$ = −3.2 cm^{-1}), which is qualitatively in agreement with other published data for aldehydes-CLF and ketones-CLF mixtures [33,34]. CLF is considered a non-polar solvent in terms of the dielectric constant value (ε_D < 5), but it is actually a low-polarity solvent (μ = 1.04 D and ε_D = 4.9) that can act as H-bond donor (α = 0.20) and presents higher values of π* and E_T(30) in comparison to CHX and TOL (Table SI.3). Previous studies on the interaction between chloroform and ketones and aldehydes provide substantial evidence that the association occurs via hydrogen bonding, Cl_3CH—O=C-R [34,35], which is possible because of the effect of electron attraction of Cl atoms on the Cl—C—H bonds. Here, the association of CLF and CNAL via hydrogen bonding would decrease the force constant of the C=O group and, as a consequence, $\nu_{C=O}$ shifts to lower frequencies. On the other hand, $\nu_{C=O}$ decreased when CNAL was dissolved in polar solvents EtOH ($\Delta\nu_{C=O}$ = −2.8 cm^{-1}), ACN ($\Delta\nu_{C=O}$ = −3.8 cm^{-1}) and 2-PrOH ($\Delta\nu_{C=O}$ = −4.8 cm^{-1}). This red shift of $\nu_{C=O}$ shows that the C=O bond of CNAL is weakened in polar solvents and reflects a strong solvation effect, due to both the solvent-induced polarization via dipole-dipole interactions and the formation of hydrogen bridges between CNAL and protic solvents EtOH and 2-PrOH. The r^0_{CNAL} values were plotted as a function of $\Delta\nu_{C=O}$ in Fig. 4 and it is apparent that there is no general relationship between r^0_{CNAL} and $\Delta\nu_{C=O}$. Nevertheless, if we take into account only the results obtained in non-polar solvents, it is observed that r^0_{CNAL} diminished with $\Delta\nu_{C=O}$, probably reflecting that the activation of carbonyl group of CNAL decreases by CNAL dilution in non-polar solvents. An opposite trend between r^0_{CNAL} and $\nu_{C=O}$ was observed in polar solvents, which may be interpreted by considering that the CNAL adsorption on surface acid sites is hindered when the CNAL-solvent interaction increases.

Table 2
Frequency shift of the $\nu_{C=O}$ absorption band of CNAL in CNAL-solvent mixtures.

CNAL-Solvent mixture	$\nu_{C=O}$ peak of CNAL Wavenumber (cm^{-1})	Frequency shift $\Delta\nu_{C=O}$ (cm^{-1})
CNAL-CNAL	1725.3	–
CNAL-CHX	1731.8	6.5
CNAL-TOL	1727.3	2.0
CNAL-EtOH	1722.5	−2.8
CNAL-CLF	1722.1	−3.2
CNAL-ACN	1721.5	−3.8
CNAL-2-PrOH	1720.5	−4.8

[T = 25 °C, C^0_{CNAL} = 0.143 M].

In summary, results in Table 2 and Fig. 4 show that the effect of solvent on catalyst activity cannot be satisfactorily interpreted only in terms of solvent-CNAL interactions as determined by $\nu_{C=O}$ band shifts. For example, r^0_{CNAL} was about 6 times higher in CLF than in EtOH in spite that the $\Delta\nu_{C=O}$ shift for citronellal was similar in both solvents. In

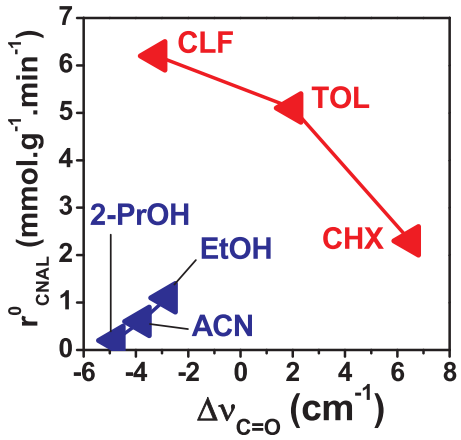

Fig. 4. Initial CNAL conversion rate as a function of the $\nu_{C=O}$ band shift of citronellal [Catalyst: SiO_2-Al_2O_3, T = 70 °C, P_{N_2} = 5 bar, W_{Cat} = 0.2 g, C^0_{CNAL} = 0.143 M, V_{CNAL}:V_{Solv} = 4:150 (mL)].

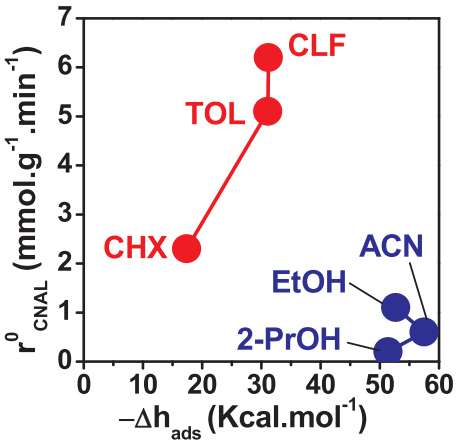

Fig. 5. Initial CNAL conversion rate as a function of solvent adsorption enthalpies [Catalyst: SiO_2-Al_2O_3, T = 70 °C, P_{N_2} = 5 bar, W_{Cat} = 0.2 g, C^0_{CNAL} = 0.143 M, V_{CNAL}:V_{Solv} = 4:150 (mL)].

order to get more insight on the effect of solvent on CNAL conversion rate we carried out additional experiments to explore the effect of solvent-catalyst interactions on catalyst activity.

3.4. Catalyst activity and solvent-catalyst interactions

Solvent-catalyst interactions were investigated by employing two different techniques: i) solvent adsorption strength was determined by measuring the solvent adsorption entalphy by calorimetry; ii) product evolution from TPD of preadsorbed solvents on SiO_2-Al_2O_3 followed by mass spectrometry furnished information on the nature and strength of solvent-catalyst interactions.

3.4.1. Study of solvent-catalyst interactions by calorimetry

The average molar adsorption enthalpies (Δh_{ads}, kcal mol^{-1}) of solvents on SiO_2-Al_2O_3 were determined by assuming a 1:1 stoichiometry between solvent molecules and acid sites, and are presented in Table 3 (the obtained experimental thermograms are shown in Fig. SI 3 and Table SI 4). The Δh_{ads} values for polar solvents were between 50 and 60 kcal mol^{-1} following the order ACN > EtOH ≅ 2-PrOH, while those corresponding to non-polar solvents were lower than 32 kcal mol^{-1}, in the order TOL ≅ CLF > CHX. These calorimetric data show that the adsorption strength of polar solvents on SiO_2-Al_2O_3 is clearly higher as compared to that of non-polar solvents.

The CNAL conversion rates as a function of Δh_{ads} are represented in Fig. 5. A general lack of correlation between r^0_{CNAL} and Δh_{ads} is observed in Fig. 5 for polar and non-polar solvents. We note that r^0_{CNAL} was higher in non-polar than in polar solvents that are strongly bonded to the catalyst surface. In contrast, if we consider only the non-polar solvents, then it is observed that the highest r^0_{CNAL} values were obtained in CLF and TOL that exhibited the highest Δh_{ads} values.

Table 3
Corrected temperature rises and solvent adsorption enthalpies over SiO_2-Al_2O_3 determined by calorimetry.

Solvent	ΔT_C (°C)	Δh_{ads} (kcal mol^{-1})
CHX	0.78	−17.4
CLF	1.39	−31.2
TOL	1.37	−31.3
2-PrOH	2.12	−51.4
EtOH	2.25	−52.7
ACN	2.45	−57.5

3.4.2. TPD of solvents on SiO_2-Al_2O_3

Fig. 6 presents the solvent TPD profiles obtained on SiO_2-Al_2O_3. In all the cases, the *m/z* signals corresponding to the most abundant fragments formed from the solvent-derived species were followed by mass spectrometry. The TPD of TOL (Fig. 6a) shows that the peak maximum corresponding to the most abundant TOL ions (*m/z* = 91, 92, 39 and 93 signals) appeared at 100 °C. An additional broad band corresponding to the evolution of C1 fragments (*m/z* = 16) was detected between 100 °C and 300 °C, with a maximum at 150 °C, and is associated with methane formed from toluene decomposition. This later result shows that a part of TOL adsorbs irreversibly on SiO_2-Al_2O_3 and decomposes at low and middle temperatures.

The desorption of CHX (Fig. 6b), followed by the *m/z* = 41, 42, 56 and 84 signals, occurred as relatively small peaks at 93 °C. No signals of evolved compounds accounting for possible decomposition of CHX molecule were detected thereby revealing a weak interaction between CHX and SiO_2-Al_2O_3, which is consistent with the fact that the CHX adsorption enthalpy was the lowest among the solvents used in this work (Table 3).

The CLF TPD curves in Fig. 6c show that CLF desorbed between 60 °C and 250 °C (*m/z* = 83, 85, 47, 48, 35) and presented two bands at 98 °C (intense) and 169 °C (weak) respectively, which suggests that a part of CLF is stronger adsorbed on SiO_2-Al_2O_3. Two additional fragment evolutions (*m/z* = 27, 70) appeared at 116 °C and 169 °C respectively, and were attributed to CH_2Cl_2 and Cl_2 formed from the dissociative chemisorption of CLF on surface acid sites of SiO_2-Al_2O_3.

Fig. 6d presents the ACN TPD profiles. The desorption of molecular ACN (*m/z* = 41) gave rise to an intense band in the 70–300 °C range with a maximum at 120 °C and a shoulder at 190 °C; other fragment evolutions (*m/z* = 39, 38, 28, 14) were also included in Fig. 6d. The evolution of the *m/z* = 41 signal indicates that there is a significant interaction between ACN and SiO_2-Al_2O_3; nevertheless, no signals of evolved compounds associated with ACN decomposition were detected.

On the other hand, the peak maximum corresponding to desorption of 2-PrOH occurred at 148 °C as shown by evolutions of the most abundant 2-PrOH fragments (*m/z* = 45, 43, 59) in Fig. 6e. Additional bands corresponding to fragments attributed to propene (*m/z* = 41, 39, 27, 42) appeared at 173 °C. Formation of propene shows that a significant part of 2-PrOH was dehydrated on the acid sites of SiO_2-Al_2O_3.

Finally, the EtOH TPD profiles are presented in Fig. 6f. Desorption of molecular EtOH (*m/z* = 31, 29, 45, 15, 46) showed a broad band between 75 °C and 320 °C with an intense peak at 110 °C and a weak one at 200 °C. Several fragments (*m/z* = 28, 27, 26) attributed to desorption of ethene formed from dehydration of EtOH presented two desorption bands at 110 °C and 285 °C, respectively.

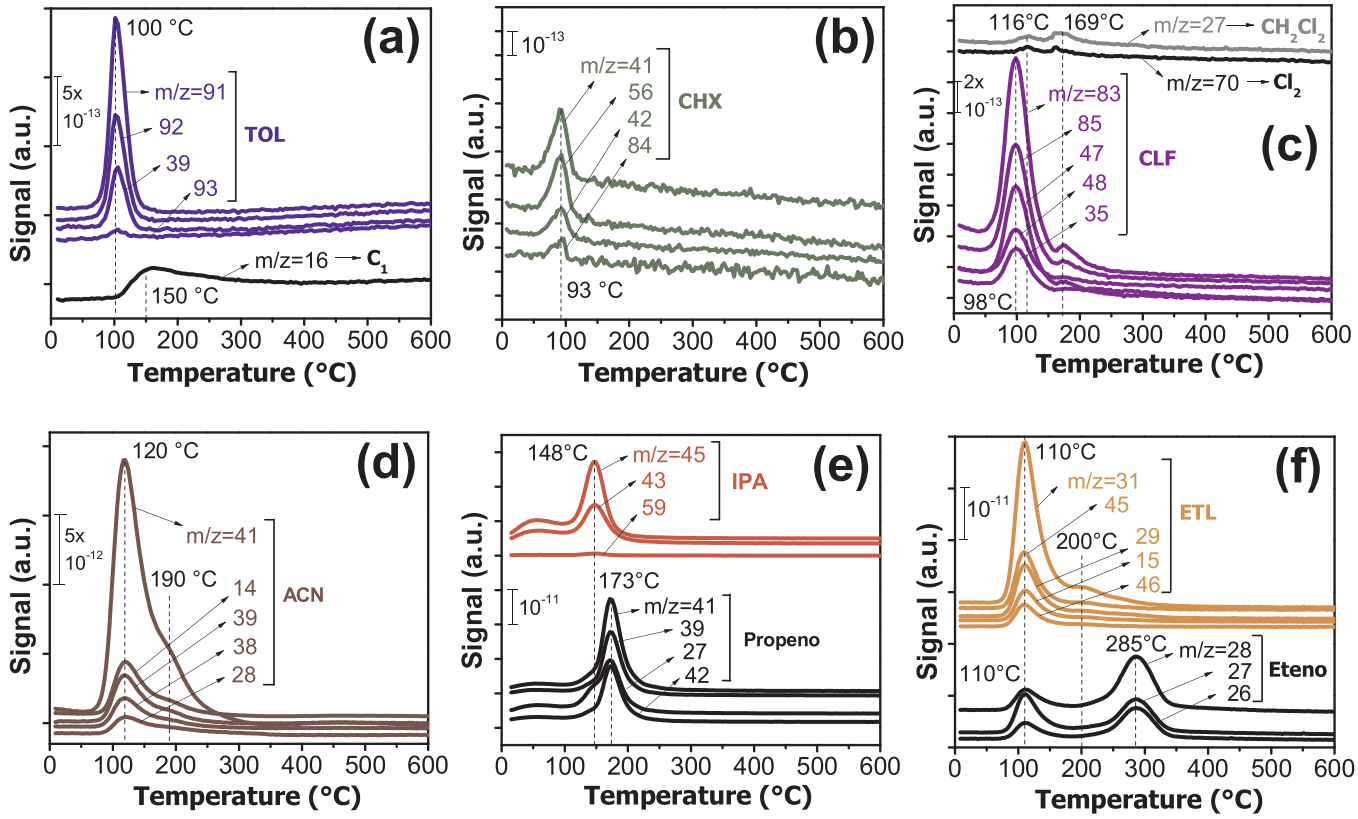

Fig. 6. TPD profiles of solvents preadsorbed at RT on SiO_2-Al_2O_3: (a) TOL; (b) CHX; (c) CLF; (d) ACN; (e) 2-PrOH; (f) EtOH [Heating rate = 10 °C min^{-1}, Ar stream = 60 mL min^{-1}, W_{Cat} = 0.15 g].

In brief, the solvent TPD curves of Fig. 6 show that the molecular desorption temperature of non-polar solvents was ≤ 100 °C while that corresponding to polar solvents was ≥ 110 °C. In agreement with the values obtained by calorimetry (Table 3), results in Fig. 6 confirm therefore the stronger interaction between polar solvents and SiO_2-Al_2O_3.

4. Discusion

The isomerization of citronellal to isopulegol is an intramolecular ene reaction, in which the C=C bond with an allylic hydrogen (the ene) of citronellal reacts with the C=O enophile group. The ene reaction is considered to proceed through a concerted mechanism via a cyclic transition state but it can also occur stepwise via cationic intermediates [36,37,38]. According to literature, the isomerization of citronellal is catalyzed by solids containing either Lewis [39,40] or Brønsted [11,14] acid sites but it seems that the reaction is more efficiently promoted on samples exhibiting dual Lewis/Brønsted acidity [13,41]. The isomerization mechanism on catalysts containing Lewis and Brønsted acid sites would involve the citronellal coordination to a strong Lewis site, followed by protonation from a neighboring Brønsted site [13]. The SiO_2-Al_2O_3 sample used in this work contains strong Lewis and weak Brønsted acid sites in a L/(L + B) ratio of 0.79, and efficiently promotes the citronellal isomerization to isopulegol. However, the citronellal conversion rate strongly depends on the solvent used in the reaction. Our results in Table 1 show, in fact, that r^0_{CNAL} was clearly lower in polar solvents EtOH, ACN and 2-PrOH than in weakly and non-polar solvents CLF, TOL and CHX. This difference in catalytic activity may be consistently explained by taking into account that the solvent TPD profiles (Fig. 6) and the data obtained by calorimetry (Table 3) showed that the adsorption strength for polar solvents on SiO_2-Al_2O_3 was stronger than for weakly and non-polar solvents. The strong adsorption of EtOH, ACN and 2-PrOH on SiO_2-Al_2O_3 suggests the existence of competitive solvent/CNAL adsorptions on surface Lewis acid sites that might decrease the number of active sites accessible for CNAL adsorption. Furthermore, our results regarding the CNAL-solvent interaction in liquid-phase (Table 2) show that CNAL is strongly solvated in polar solvents. The CNAL molecules would be then surrounded by solvent molecules that hinder the CNAL adsorption on surface acid sites, thereby contributing to decrease the catalyst activity. On the other hand, the selectivity to isopulegol and the carbon balance were clearly lower in polar protic solvents EtOH and 2-PrOH than in the other solvents (Table 1). Previous works on citronellal isomerization over Ru(Pt)/C catalysts have reported the formation of citronellal acetals when the reaction is conducted in alcohols such as ethanol or 2-PrOH, thereby decreasing significantly the selectivity to isopulegol [42,43]. Similarly, the reaction of CNAL with EtOH or 2-PrOH on the acid sites of SiO_2-Al_2O_3 to form citronellal acetals may explain here the lower selectivity to isopulegol observed when the reaction was performed in these alcohols. Nevertheless, we did not detect acetals in the liquid phase, probably because the acetal intermediates remained adsorbed on the catalyst surface, which is consistent with the low carbon balance values determined in alcohols (%C = 62.9% in EtOH, Table 1). In order to verify this assumption, we carried out additional catalytic tests for quantifying the amount of coke formed on SiO_2-Al_2O_3 when the CNAL isomerization reaction is carried out in EtOH. Specifically, the carbon deposited on SiO_2-Al_2O_3 following a standard CNAL isomerization run in EtOH (5 h at 70 °C) was characterized by TPO technique and compared with the carbon formed after contacting a SiO_2-Al_2O_3 sample only with EtOH under the same experimental conditions (blank run). Results are presented in Fig. 7. The TPO curve corresponding to the SiO_2-Al_2O_3 sample recovered from the blank run in EtOH exhibited two small peaks at 290 °C and 563 °C, respectively, while that the sample recovered after the CNAL isomerization run in EtOH presented an additional large peak at 158 °C that reveals the formation of citronellal-derived coke deposits. The carbon contents determined from the areas

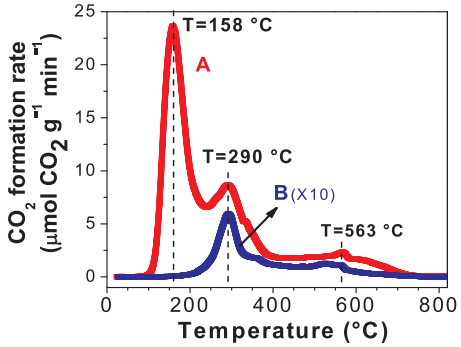

Fig. 7. TPO profiles of SiO_2-Al_2O_3 samples recovered after the citronellal isomerization run in EtOH (A) and the blank run in EtOH (B) [5 h at 70 °C].

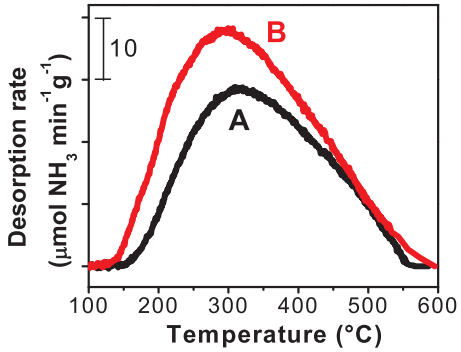

Fig. 8. TPD of NH_3 adsorbed at 100 °C on SiO_2-Al_2O_3 (A) and SiO_2-Al_2O_3 contacted with chloroform (B) [30 min at 70 °C].

under the curves of Fig. 7 were 0.6% (blank run) and 23.3% (CNAL isomerization run). The significant amounts of coke formed during the CNAL isomerization in EtOH is consistent then with the assumption that CNAL can react with EtOH forming byproducts such as acetals that remain adsorbed on SiO_2-Al_2O_3 and diminishing the selectivity to the formation of isopulegol.

SiO_2-Al_2O_3 efficiently promotes the selective synthesis of isopulegol from citronellal in weakly and non-polar solvents CLF, TOL and CHX; the selectivity to isopulegol was in fact ≥ 97.7% in the three solvents (Table 1). Regarding the SiO_2-Al_2O_3 activity, the CNAL conversion rate followed the order CLF > TOL > CHX. TOL and CHX are not H-bond donor solvents and they interact with CNAL in liquid phase only via dispersion forces (dilution effect) without forming any type of H-bonds with CNAL. Here, we observed that the vibration frequency of the C=O group of CNAL increases following the CNAL dilution in TOL or CHX (Table 2). These $\nu_{C=O}$ upward shifts are explained by considering that the interaction between CNAL and TOL or CHX is very weak, so that the main solvent effect is to decrease the interaction between CNAL molecules, which increases the force constant of the carbonyl group. Nevertheless, $\Delta\nu_{C=O}$ was much higher in CHX (6.5 cm^{-1}) than in TOL (2.0 cm^{-1}) indicating a weaker solvent/CNAL interaction when CNAL is dissolved in CHX, which is consistent with the fact that the polarity/polarizability index π* is zero for CHX (Table SI.3). The lower activation of the C=O group of CNAL in CHX may explain then that the citronellal conversion rate on SiO_2-Al_2O_3 was lower in CHX than in TOL. It is worth noting that the CHX adsorption strength on SiO_2-Al_2O_3 as determined in our TPD experiments (Fig. 6) was very weak and is not expected, therefore, that the interaction CHX/catalyst can influence the intrinsic kinetics of the citronellal conversion to isopulegol on surface acid sites.

The highest SiO_2-Al_2O_3 activity for CNAL conversion was obtained in CLF. Our results show that a strong interaction exits between CNAL and CLF in liquid phase, probably via hydrogen bonding, which would hinder the CNAL adsorption on the catalytic surface by the solvation effect. The high activity observed for SiO_2-Al_2O_3 in CLF cannot be explained then by any CNAL-CLF interaction in liquid phase. The TPD profiles of CLF on SiO_2-Al_2O_3 showed that a part of CLF is dissociatively chemisorbed on the solid and releases CH_2Cl_2 and Cl_2 to the gas phase (Fig. 6c). Probably, chlorinated species formed from CLF decomposition may remain on the catalyst and generate additional surface acid sites that would enhance the catalyst activity. In order to verify this assumption, we performed additional experiments by measuring the SiO_2-Al_2O_3 acidity following CLF adsorption. Specifically, a SiO_2-Al_2O_3 sample was impregnated with CLF for 30 min at the reaction temperature (70 °C) and then treated in Ar at 200 °C for 30 min to eliminate physisorbed CLF. The sample acidity was then determined by ammonia TPD and the results are presented in Fig. 8. The NH_3 surface densities for acid sites were determined by deconvolution and integration of TPD traces of Fig. 8. A value of 456 μmol g^{-1} was obtained for SiO_2-Al_2O_3 sample pretreated with CLF, which is about 20% higher as compared to SiO_2-Al_2O_3 reference sample (380 μmol g^{-1}). These results that show that the SiO_2-Al_2O_3 acidity is enhanced by CLF impregnation at the reaction temperature may explain therefore that the highest CNAL isomerization rate was determined here in chloroform.

5. Conclusions

The SiO_2-Al_2O_3 activity and selectivity for the acid-catalyzed isomerization of citronellal to isopulegol greatly depend on the solvent used. The catalyst activity in polar solvents (ethanol, acetonitrile, 2-propanol) is lower than in weakly and non-polar solvents (chloroform, toluene, cyclohexane), mainly because polar solvents strongly adsorb on the catalyst surface and partially block the acid active sites for reactant adsorption. Furthermore, the strong CNAL-polar solvent interaction increases the CNAL solvation in liquid phase and thereby hinders the CNAL adsorption on SiO_2-Al_2O_3, which contributes to decreasing the CNAL conversion rate. The selectivity to isopulegol was lower in polar protic alcohols (EtOH and 2-PrOH), because CNAL react with these solvents forming byproducts that remain adsorbed on the catalyst surface.

In weakly and non-polar solvents, SiO_2-Al_2O_3 forms selectively isopulegol from citronellal; the selectivity to isopulegol in CLF, TOL and CHX was in fact ≥ 97.7%. The SiO_2-Al_2O_3 activity for CNAL isomerization follows the order CLF > TOL > CHX. TOL and CHX are not H-bond donor molecules and they interact with CNAL in liquid phase only via dispersion forces (dilution effect). The adsorption strength of non-polar solvents on SiO_2-Al_2O_3 was clearly lower as compared to polar solvents; in particular, the interaction between CHX and SiO_2-Al_2O_3 was very weak. The highest CNAL conversion rate was obtained in CLF. Chloroform is dissociatively chemisorbed on SiO_2-Al_2O_3 and releases CH_2Cl_2 and Cl_2 to the gas phase. Additional surface acid sites are generated from CLF decomposition, thereby increasing the SiO_2-Al_2O_3 acidity and enhancing its catalytic activity.

Acknowledgements

The authors gratefully acknowledge the Universidad Nacional del Litoral (UNL; Grant CAI+D 50020110100019), Consejo Nacional de Investigaciones Científicas y Técnicas (CONICET; Grant PIP-767-2015), and Agencia Nacional de Promoción Científica y Tecnológica (ANPCyT; Grant PICT-2011-0419), Argentina, for the financial support of this work.

Appendix A. Supplementary data

Supplementary material related to this article can be found, in the online version, at doi:https://doi.org/10.1016/j.mcat.2018.09.009.

References

[1] P.N. Rylander, Catalytic Hydrogenation Over Platinum Metals, Academic Press, New York, 1967.
[2] L. Hegedus, T. Máthé, T. Kárpáti, Appl. Catal. A 349 (2008) 40–45.
[3] M. Besson, J.M. Bonnier, M. Joucla, Bull. Soc. Chim. France 127 (1990) 5–12.
[4] N.M. Bertero, A.F. Trasarti, C.R. Apesteguía, A.J. Marchi, Appl. Catal. A Gen. 394 (2011) 228–238.
[5] A.F. Trasarti, N.M. Bertero, C.R. Apesteguía, A.J. Marchi, Appl. Catal. A Gen. 475 (2014) 282–291.
[6] D.J. Segobia, A.F. Trasarti, C.R. Apesteguía, Catal. Sci. Technol. 4 (2014) 4075–4083.
[7] D.J. Segobia, A.F. Trasarti, C.R. Apesteguía, J. Braz. Chem. Soc. 25 (2014) 2272–2279.
[8] D.J. Segobia, A.F. Trasarti, C.R. Apesteguía, Catal. Commun. 62 (2015) 62–66.
[9] C. Milone, C. Gangemi, G. Neri, A. Pistone, S. Galvagno, Appl. Catal. A Gen. 199 (2000) 239–244.
[10] A.F. Trasarti, A.J. Marchi, C.R. Apesteguía, J. Catal. 224 (2004) 484–488.
[11] M. Fuentes, J. Magraner, C. De Las Pozas, R. Roque-Malherbe, J. Perez Pariente, A. Corma, Appl. Catal. 47 (1989) 367–374.
[12] N. Ravasio, M. Antenori, F. Babudri, M. Gargano, Stud. Surf. Sci. Catal. 108 (1997) 625–632.
[13] G.D. Yadav, J.J. Nair, Langmuir 16 (2000) 4072–4079.
[14] G.K. Chuah, S.H. Liu, S. Jaenicke, L.J. Harrison, J. Catal. 200 (2001) 352–359.
[15] K.A. da Silva, P.A. Robles-Dutenhefner, E.M.B. Sousa, E.F. Kozhevnikova, I.V. Kozhevnikov, E.V. Gusevskaya, Catal. Commun. 5 (2004) 425–429.
[16] A.F. Trasarti, A.J. Marchi, C.R. Apesteguia, J. Catal. 247 (2007) 155–165.
[17] M. Vandichel, F. Vermoortele, S. Cottenie, D.E. De Vos, M. Waroquier, V. Van Speybroeck, J. Catal. 305 (2013) 118–129.
[18] S.M. Coman, P. Patil, S. Wuttke, E. Kemnitz, Chem. Commun. (2009) 460–462.
[19] P. Müller, P. Wolf, I. Hermans, ACS Catal. 6 (2016) 2760–2769.
[20] Z. Yongzhong, N. Yuntong, S. Jaenicke, G.K. Chuah, J. Catal. 229 (2005) 404–413.
[21] H.C. Dickinson, Bull. Bur. Stand. II (1915) 189–257.
[22] P.A. Ramachandran, R.V. Chaudhari, Three-Phase Catalytic Reactors, Gordon and Breach Science Publishers, 1983.
[23] P.B. Weisz, C.D. Prater, Adv. Catal. 6 (1954) 143–196.
[24] J.W. Ward, J. Catal. 10 (1968) 34–46.
[25] G. Busca, Catal. Today 41 (1998) 191–206.
[26] Y. Marcus, Chem. Soc. Rev. 22 (1993) 409–416.
[27] C. Reidchardt, Solvents and Solvent Effects in Organic Chemistry, third ed., Wiley VCH, New York, 2004.
[28] M.J. Kamlet, J.L.M. Abboud, M.H. Abraham, P.L. Grellier, R.M. Doherty, R. Taft, Can. J. Chem. 66 (1988) 2673–2686.
[29] E.M. Kosower, J. Am. Chem. Soc. 80 (1958) 3253–3260.
[30] E.J. Hartwell, R.E. Richards, H.W. Thompson, J. Chem. Soc. (1948) 1436–1441.
[31] M.L. Josien, J. Lascombe, J. Chim. Phys. 52 (1955) 162.
[32] L.J. Bellamy, R.L. Williams, Proc. R. Soc. Lond. A 255 (1960) 22–32.
[33] K.B. Whetsel, R.E. Kagarise, Spectrochim. Acta 18 (1962) 329–339.
[34] J.S. Byrne, P.F. Jackson, K.J. Morgan, J. Chem. Soc. Perkin Trans. 2 (1972) 1291–1295.
[35] E.R. Kearns, J. Phys. Chem. 65 (1961) 314–339.
[36] W. Oppolzer, V. Snieckus, Angew. Chemie – Int. Ed. English 17 (1978) 476–486.
[37] K. Mikami, M. Shimizu, Chem. Rev. 92 (1992) 1021–1050.
[38] M.L. Clarke, M.B. France, Tetrahedron 64 (2008) 9003–9031.
[39] C. Milone, A. Perri, A. Pistone, G. Neri, S. Galvagno, Appl. Catal. A: Gen. 233 (2002) 151–157.
[40] A. Corma, M. Renz, Chem. Commun. (2004) 550–551.
[41] A.F. Trasarti, A.J. Marchi, C.R. Apesteguía, Catal. Commun. 32 (2013) 62–66.
[42] P. Mäki-Arvela, L.P. Tiainen, A.K. Neyestanaki, R. Sjöholm, T.K. Rantakylä, E. Laine, T. Salmi, D. Yu, Murzin, Appl. Catal. A: Gen. 237 (2002) 181–200.
[43] I.M.J. Villela, S.R. de Miguel, O.A. Scelza, Latin Amer. Appl. Res. 35 (2005) 51.